X-ray Structures and DFT Calculations on Rhodium−Olefin Complexes: Comments on the ^{103}Rh NMR Shift−Stability Correlation

Michael Bühl,*,† Mikael Håkansson,‡ Amir H. Mahmoudkhani,§ and Lars Öhrström*,‡

Max-Planck-Institut für Kohlenforschung, Kaiser-Wilhelm-Platz 1, D-45470 Mülheim an der Ruhr, Germany, Department of Inorganic Chemistry, Chalmers Tekniska Högskola, SE-412 96 Gothenburg, Sweden, and Department of Chemistry, Gothenburg University, SE-412 96 Gothenburg, Sweden

Received May 18, 2000

The low-temperature X-ray structures of bis(η^2-ethene)(2,4-pentanedionato)rhodium(I) (**1**)- and bis(η^2-ethene)(1,1,1,5,5,5-hexafluoro-2,4-pentanedionato)rhodium(I) (**2**) were determined. Very similar Rh−ethene coordination geometries are found in the solid state, i.e., **1**, Rh−C = 2.127(5) Å, and **2**, Rh−C = 2.121(3) Å, in good accord with DFT calculations, i.e., **1**, Rh−C = 2.132 Å, and **2**, Rh−C = 2.136 Å. The calculated ^{103}Rh NMR chemical shifts (GIAO-B3LYP/II level) for a range of bis(η^2-alkene)(2,4-pentanedionato)rhodium(I) complexes also agree well with solution NMR data. The empirical correlation between transition-metal shifts and stability constants (Öhrström, L. *Comm. Inorg. Chem.* **1996**, *18*, 305) could be confirmed for simple alkenes, since the computed relative Rh−alkene binding energies were found to correlate with δ(^{103}Rh). In contrast, chelating or fluorinated alkenes showed large deviations from this correlation. The steric and electronic effects on the Rh−alkene bond are discussed and analyzed in terms of Bader's atoms-in-molecules theory, which revealed qualitatively different binding modes of ethene and tetrafluoroethene to rhodium: ethene forms typical π-complexes in the Dewar−Chatt−Duncanson model, whereas tetrafluoroethene complexes are on the borderline to metallacyclopropanes.

Introduction

Transition-metal ethene chemistry can be regarded as the starting point of organometallic chemistry[1] and has recently focused on new transition-metal-based catalysts for ethene polymerization.[2] Low-temperature X-ray measurements are needed to get detailed structural information on the metal−alkene bond since the small ethene ligand is close to a metal center with high electron density and also in many cases rotates fairly easily. Even so, it is somewhat surprising that no detailed structure has been published for one of the most intensely studied rhodium−ethene complexes,[3] Cramer's compound, Rh(acac)(ethene)$_2$,[4,5] or its hexafluoro derivative, Rh(hfacac)(ethene)$_2$. This is the subject of the first part of this paper.

Scheme 1

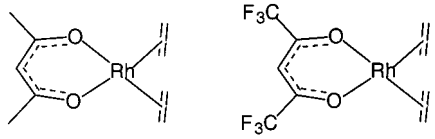

1 **2**

Because of the somewhat peculiar bond mode of the ethene ligand to the metal center,[6] and the industrial importance of this chemistry, quantum chemical calculations on these compounds have interested theoreticians ever since such computations were first feasible.[7] The subject of the second part of this paper is to evaluate the accuracy of modern density functional theory (DFT) in describing the structures of rhodium−alkene complexes. The use of DFT to compute structures, energetics, and spectroscopic properties of transition-metal

* Corresponding authors. M.B.: fax +49-208-306 2996, e-mail buehl@mpi-muelheim.mpg.de. L.Ö.: fax +46 31 772 28 46, e-mail ohrstrom@inoc.chalmers.se.
† Max Planck Institut.
‡ Chalmers.
§ Gothenburg University.

(1) The synthesis of K[PtCl$_3$(C$_2$H$_4$)]: Zeise, W. C. *Ann. Phys.* **1827**, *9*, 932.

(2) For example: (a) Held, A.; Bauers, F. M.; Mecking, S. *Chem. Commun.* **2000**, 301−302. (b) Small, B. L.; Brookhart, M. *Macromolecules* **1999**, *32*, 2120−2130. (c) Britovsek, G. J. P.; Gibson, V. C.; Kimberley, B. S.; Maddox, P. J.; McTavish, S. J.; Solan, G. A.; White, A. J. P.; Williams, D. J. *Chem. Commun.* **1998**, 849−850.

(3) See references in: Åkermark, B.; Glaser, J.; Öhrström, L.; Zetterberg, K. *Organometallics* **1991**, *10*, 733−736. acac = 2,4-pentanedionato, hfacac = 1,1,1,5,5,5-hexafluoro-2,4-pentanedionato.

(4) Cramer, R. *J. Am. Chem. Soc.* **1964**, *86*, 217−222.

(5) X-ray diffraction: (a) Evans, J. A.; Russell, D. R. *J. Chem. Soc., Chem. Commun.* **1971**, 197−198. Room-temperature, preliminary communication: (b) Vierkötter, S. A.; Barnes, C. E.; Garner, G. L.; Butler, L. G. *J. Am. Chem. Soc.* **1994**, *116*, 7445−7446. Low-temperatue, only Rh−C distance reported.

(6) The Dewar−Chatt−Duncanson model: (a) Dewar, M. J. S. In *Colloque international sur les réarrangements moléculaires et l'inversion de Walden*; Montpellier, 1950; Mousseron, M., Ed. In *Bull. Soc. Chim. Fr.* **1951**, *18*, C79. (b) Chatt, J.; Duncansson, L. A. *J. Chem. Soc.* **1953**, 2939. (c) Chatt, J.; Duncanson, L. A. In *Symposium on coordination chemistry*; Danish Chemical Society: Copenhagen, 1953; p 112.

(7) For example: (a) Armstrong, D. R.; Perkins, P. G.; Stewart, J. J. P. *J. Chem. Soc., Dalton Trans.* **1972**, 1972−1980. (b) Cossee, P. *J. Catal.* **1964**, *3*, 80−88. (c) Åkermark, B.; Almemark, M.; Almlöf, J.; Bäckvall, J.-E.; Roos, B.; Stögård, Å. *J. Am. Chem. Soc.* **1977**, *99*, 4617−4624.

10.1021/om000419y CCC: $19.00
Publication on Web 11/16/2000

compounds is now well established.[8] Furthermore, as the methods of calculating metal NMR chemical shifts now seem to have attained a reliable level,[9−15] we wanted to investigate the empirical correlation between transition-metal shifts and stablility constants[16−18] by the calculation of Rh-shifts and binding energies for a series of Rh(acac)(alkene)$_2$ complexes.

This aspect of our work goes well beyond metal−alkene chemistry since transition-metal NMR is finding increased use among organometallic and coordination chemists, while the interpretation of metal NMR shifts in terms of physical properties is not straightforward.[19] The metal NMR chemical shifts have been correlated with a number of properties, most notably maybe with catalytic activity,[11,20] but a thorough understanding of why these dependencies exist is needed before they can be exploited by the practicing chemist.

Experimental Section

Reagents and Solvents. All reagents were purchased from commercial sources and used without further purification. Rh($C_5H_7O_2$)(C_2H_4)$_2$ (**1**) and Rh($C_5HF_6O_2$)(C_2H_4)$_2$ (**2**) were prepared according to the literature.[21] **1** was recrystallized from *n*-hexane and **2** from diethyl ether.

X-ray Crystallography. Crystal and experimental data are summarized in Table 1. For Rh($C_5H_7O_2$)(C_2H_4)$_2$, **1**, diffracted intensities were measured at −120 °C using a Rigaku AFC6 diffractometer and graphite-monochromated Mo Kα (0.71073 Å) radiation from a RU200 rotating anode source operated at 9 kW (50 kV; 180 mA). The $\omega/2\theta$ scan mode was employed, and stationary background counts were recorded on each side of the reflection, the ratio of peak counting time vs background counting time being 2:1. In the $5° < 2\theta < 50°$ interval 901 unique reflections were measured for a yellow crystal with approximate dimensions 0.15 × 0.15 × 0.15 mm, using an ω scan rate of 16°/min and a scan width of $(0.89 + 0.30 \times \tan\theta)°$. The intensities of three reflections monitored regularly after measurement of 150 reflections indicated crystal stability during data collection. Correction was made for Lorentz and polarization effects, and an empirical correction based on azimutal scans for several reflections was made for the effects of absorption (minimum/maximum transmission factors = 0.907/0.966). Cell constants were obtained by least-squares refinement from the setting angles of 20 reflections in the range $14.4° < 2\theta < 16.9°$. The structure was solved by direct methods and subsequent full-matrix least-squares refinement, including anisotropic thermal parameters for all non-hydrogen. The hydrogen atoms were located from difference Fourier maps and refined isotropically. The calculations were carried out with the SHELXS-86 and SHELXL-93[22] program packages.

For Rh($C_5HF_6O_2$)(C_2H_4)$_2$ (**2**), diffracted intensities were measured using a Siemens SMART CCD diffractometer (graphite-monochromated Mo Kα (0.71073 Å) radiation) equipped with a Siemens LT-2A low-temperature device at −90 °C. More than a hemisphere of the reciprocal lattice was scanned by 0.3° steps in ω with a crystal-to-detector distance of 3.97 cm and exposure time of 10 s per frame. A preliminary orientation matrix was obtained from the first frames using SMART.[23] The collected frames were integrated using the preliminary orientation matrix, which was updated every 100 frames. Final cell parameters were obtained by refinement on the positions of 3778 reflections with $I > 10\sigma(I)$ after integration of all the frames of data using SAINT.[23] The data were empirically corrected for absorption and other effects using SADABS[24] (min./max. transmission = 0.7944/0.8638) based on the method of Blessing.[25] The structure was solved by direct methods and subsequent full-matrix least-squares refinement on all data

Table 1. Selected Crystallographic Data for 1 and 2

	1: C9 H15 O2 Rh	**2:** C9 H9 F6 O2 Rh
formula		
fw	258.12	366.07
temp, K	153 K	183(2) K
color and habit	yellow block	orange block
cryst syst	orthorhombic	orthorhombic
space group	P_{nma}	P_{nma}
a, Å	7.6496(12)	16.9179(3)
b, Å	14.278(3	8.20150(1)
c, Å	9.039(2)	8.5513(2)
volume, Å^3	987.2(3)	1186.51(3)
Z	4	4
density (calc), g cm^3	1.737	2.049
cryst dimens, mm	0.15 × 0.15 × 0.15	0.12 × 0.10 × 0.08
μ, mm^{-1}	1.689	1.508
F(000)	520	712
θ range for data collectn	2.67−25.01°	2.41−30.50°
limiting indices	$0 \le h \le 9$	$-18 \le h \le 24$
	$0 \le k \le 16$	$-11 \le k \le 11$
	$-10 \le l \le 0$	$-12 \le l \le 12$
no. of reflns collected/ unique	901/668	11 158/1927
R(int)		0.0727
max. and min. transmn	0.966 and 0.907	0.8889 and 0.8398
no. of data/restraints/ params	668/0/89	1927/0/116
goodness-of-fit on F^2	0.740	1.045
no. of obsd reflns	668 ($I > 2\sigma(I)$)	1425 ($I > 2\sigma(I)$)
final *R* indices [$I > 2\sigma(I)$]	R1 = 0.0253, wR2 = 0.0733	R1 = 0.0421, wR2 = 0.0773
R indices (all data)	R1 = 0.0517, wR2 = 0.0991	R1 = 0.0704, wR2 = 0.0882
largest diff peak and hole, e/Å^3	0.451 and −0.612	0.543 and −0.829

(8) (a) Davidson, E. R. *Chem. Rev* **2000**, *100*. Note the following quote from the foreword: "Computational transition metal chemistry today is almost synonymous with DFT for medium-sized molecules.", pp 351−552. (b) Koch, W.; Holthausen, M. C. *A Chemist's Guide to Density Functional Theory*; Wiley-VCH: Weinheim, 2000, and the extensive bibliography therein.

(9) Bühl, M. *Chem. Phys. Lett.* **1997**, *267*, 251−257.

(10) Bühl, M. *Organometallics* **1997**, *16*, 261−267.

(11) Bühl, M. *Angew. Chem. Int. Ed.* **1998**, *37*, 142−144.

(12) Bühl, M.; Hamprecht, F. A. *J. Comput. Chem.* **1998**, *19*, 113−122.

(13) Bühl, M. *Chem.-Eur. J.* **1999**, *5*, 3514−3522.

(14) (a) Bühl, M.; Kaupp, M.; Malkina, O. L.; Malkin, V. G. *J. Comput. Chem.* **1999**, *20*, 91−105. (b) Donkervoort, J. G.; Bühl, M.; Ernsting, J. M.; Elsevier, C. J. *Eur. J. Inorg. Chem.* **1999**, 27−33. (c) Schrenkenbach, G.; Ziegler, T. *Theor. Chem. Acc.* **1998**, *99*, 71−81.

(15) Leitner, W.; Bühl, M.; Fornika, R.; Six, C.; Baumann, W.; Dinjus, E.; Kessler, M.; Kruger, C.; Rufinska, A. *Organometallics* **1999**, *18*, 1196−1206.

(16) Åkermark, B.; Blomberg, M.; Glaser, J.; Öhrström, L.; Wahlberg, S.; Wärnmark, K.; Zetterberg, K. *J. Am. Chem. Soc.* **1994**, *116*, 3405−3413.

(17) Read, M. C.; Glaser, J.; Persson, I.; Sandström, M. *J. Chem. Soc., Dalton Trans.* **1994**, 3243−3248.

(18) Öhrström, L. *Comm. Inorg. Chem.* **1996**, *18*, 305−323.

(19) (a) Pregosin, P. S., Ed. *Transition Metal Nuclear Magnetic Resonance*; Elsevier: Amsterdam, 1991. (b) v. Philipsborn, W. *Chem. Soc. Rev.* **1999**, 95−106.

(20) (a) Bönnemann, H.; Brijoux, W.; Brinkmann, R.; Meurers, W.; Mynott, R.; Philipsborn, W. v.; Egolf, T. *J. Organomet. Chem.* **1984**, *272*, 231. (b) DeShong, P.; Slough, G. A.; Sidler, D. R.; Rybczynski, P. J.; Philipsborn, W. v.; Kunz, R. W.; Bursten, B. E.; Clayton, T. W. J. *Organometallics* **1989**, *8*, 1381−1388. (c) Fornika, R.; Görls, H.; Seeman, B.; Leitner, W. *J. Chem. Soc., Chem. Commun.* **1995**, 1479−1480.

(21) (a) Cramer, R. *Inorg. Synth.* **1974**, *15*, 15−18. (b) Dam, H. v.; Terpstra, A.; Stufkens, D. J.; Oskam, A. *Inorg. Chem.* **1980**, *19*, 3448−3455.

(22) SHELEXS: Sheldrick, G. M. *Acta Crystallogr.* 1990, A, 467. SHELX-93: Sheldrick, G. M. Universität Göttingen, 1993.

(23) SMART and SAINT: Area detector control and integration software; Siemens analytical X-ray Instruments Inc.: Madison, WI, 1995.

(24) SADABS: Program for empirical absorption correction of area detectors; Sheldrick, G. M. University of Göttingen: Göttingen, Germany, 1996.

(25) Blessing, R. H. *Acta Crystallogr. Sect. A* **1995**, *51*, 33−38.

using SHELXTL.[26] The non-hydrogen atoms were refined anisotropically. The hydrogen atoms were located from difference Fourier maps and refined isotropically.

Computational Details. Methods and basis sets correspond to those used in the previous studies of second-row transition-metal complexes:[9,10,13−15,27] Geometries have been fully optimized in the given symmetry at the BP86/ECP1 level, i.e., employing the exchange and correlation functionals of Becke[28] and Perdew,[29] respectively, together with a fine integration grid (75 radial shells with 302 angular points per shell) and the weighting scheme according to Becke,[30] a relativistic MEFIT effective core potential with the corresponding valence basis sets for Rh (contraction scheme [6s5p3d]),[31] and standard 6-31G* basis set[32] for all other elements. Harmonic frequencies have been computed numerically or analytically and have been used for the evaluation of zero-point energies (ZPEs) and thermodynamic functions.

Magnetic shieldings σ have been evaluated for the BP86/ECP1 geometries using a recent implementation of the GIAO (gauge-including atomic orbitals)-DFT method,[33] involving the functional combinations according to Becke (hybrid)[34] and Lee, Yang, and Parr[35] (denoted B3LYP), together with basis II, i.e., a [16s10p9d] all-electron basis for Rh, contracted from the well-tempered 22s14p12d set of Huzinaga and Klobukowski[36] and augmented with two d-shells of the well-tempered series, and the recommended IGLO-basis II[37] on all other atoms. The σ values have been converted into chemical shifts δ (relative to the standard frequency $\Xi = 3.15$ MHz with $\delta(^1H)$ of $SiMe_4$ at 100 MHz)[38] using σ(standard) = −878, as derived in ref 9.

Reaction energies, ΔE, are reported at the B3LYP/II level employing BP86/ECP1 geometries and have been converted into reaction enthalpies ΔH and free energies ΔG at 298 K using ZPEs, heat capacities, and entropies from unscaled BP86/ECP1 harmonic frequencies, together with standard statistical procedures.[39] In addition, for selected compounds topological analyses of the B3LYP/II total electron density have been performed according to the atoms-in-molecules theory,[40] and bond orders have been computed employing natural population analysis (NPA)[41] using Wiberg's definition.[42] All computations have been performed using the Gaussian suite of programs,[43] except for the topological analyses, which employed the Morphy program.[44]

Table 2. Selected Bond Lengths [Å] and Angles [deg] for Rh(acac)(ethene)$_2$, 1

Rh(1)−O(1)	2.051(4)	O(1)−Rh(1)−O(1)	90.9(2)
Rh(1)−C(3)	2.129(5)	C(3)−Rh(1)−C(3)	89.2(3)
Rh(1)−C(4)	2.125(6)	C(3)−Rh(1)−C(4)	37.6(2)
O(1)−C(1)	1.279(6)	O(1)−C(1)−C(2)	126.1(5)
C(1)−C(2)	1.397(6)	O(1)−C(1)−C(5)	114.7(4)
C(1)−C(5)	1.512(7)	C(2)−C(1)−C(5)	119.2(5)
C(3)−C(4)	1.372(8)	C(1)−C(2)−C(1)	126.9(7)
		Rh(1)−C(3)−H(6)	112(3)
		Rh(1)−C(3)−H(5)	110(4)
		Rh(1)−C(4)−H(8)	109(3)
		Rh(1)−C(4)−H(7)	109(4)

Table 3. Selected Bond Lengths [Å] and Angles [deg] for Rh(hfacac)(ethene)$_2$, 2

Rh(1)−O(2)	2.064(3)	O(2)−Rh(1)−O(1)	89.97(13)
Rh(1)−O(1)	2.078(3)	C(1)−Rh(1)−C(1)	38.1(2)
Rh(1)−C(1)	2.118(3)	C(1)−Rh(1)−C(2)	89.16(18)
Rh(1)−C(2)	2.124(4)	C(2)−Rh(1)−C(2)	37.7(2)
O(2)−C(3)	1.255(6)	C(3)−C(4)−C(5)	123.4(4)
O(1)−C(5)	1.254(5)	O(1)−C(5)−C(4)	129.3(4)
C(6)−C(5)	1.542(6)	O(2)−C(3)−C(4)	129.2(5)
C(4)−C(3)	1.389(6)	Rh(1)−C(2)−H(22)	112(2)
C(4)−C(5)	1.393(6)	Rh(1)−C(2)−H(21)	107(2)
C(3)−C(7)	1.527(7)	Rh(1)−C(1)−H(12)	108(2)
C(2)−C(2)	1.372(8)	Rh(1)−C(1)−H(11)	115(3)
C(1)−C(1)	1.383(8)		

Results

X-ray Structure Description of 1 and 2. Crystallographic data are given in Table 1, and selected interatomic distances and angles are collected in Table 2 and Table 3. The molecular structures are depicted in Figure 1. The two molecules crystallize in the same space group but are not isomorphic. The crystal packing of **1** is herringbone-like, whereas in **2** the complexes are stacked in columns with a Rh−Rh separation of 4.123 ± 0.005 Å and a Rh−Rh−Rh angle of 168 ± 1°. The hydrogens were located on the difference Fourier maps, and the nonplanarity of the ethene ligands is evident from the *trans*-H−C−C−H dihedral angles, 156 ± 6° for **1** and 154 ± 6° for **2**.

DFT Calculations of Rh(acac)(alkene)$_2$ Complexes. Selected interatomic distances and angles for the optimized structures of **1** and **2** are given in Table 4. Calculated energies for the exchange of one or both ethenes for other alkenes or diolefins in Rh(acac)(ethene)$_2$ are reported in Table 5. The computed energies were very similar (typically within 1 kcal/mol) at the two levels employed, BP86/ECP1 and B3LYP/II,

(26) SHELXTL 5.10: Bruker AXS Inc.: Madison, WI, 1997.
(27) Bühl, M.; Baumann, W.; Kadyrov, R.; Borner, A. *Helv. Chim. Acta* **1999**, *82*, 811−820.
(28) Becke, A. D. *Phys. Rev. A* **1988**, *38*, 3098−3100.
(29) (a) Perdew, J. P. *Phys. Rev. B* **1986**, *33*, 8822−8824. (b) Perdew, J. P. *Phys. Rev. B* **1986**, *34*, 7406.
(30) Becke, A. D. *J. Chem. Phys.* **1988**, *88*, 2547.
(31) Andrae, D.; Häussermann, U.; Dolg, M.; Stoll, H.; Preuss, H. *Theor. Chim. Acta* **1990**, *77*, 123−141.
(32) (a) Hehre, W. J.; Ditchfield, R.; Pople, J. A. *J. Chem. Phys.* **1972**, *56*, 2257−2261. (b) Hariharan, P. C.; Pople, J. A. *Theor. Chim. Acta* **1973**, *28*, 213−222.
(33) Cheeseman, J. R.; Trucks, G. W.; Keith, T. A.; Frisch, M. J. *J. Chem. Phys.* **1996**, *104*, 5497−5509.
(34) Becke, A. D. *J. Chem. Phys.* **1993**, *98*, 5648−5642.
(35) Lee, C.; Yang, W.; Parr, R. G. *Phys. Rev. B* **1988**, *37*, 785−789.
(36) Huzinaga, S.; Klobukowski, M. *J. Mol. Struct.* **1988**, *167*, 1−210.
(37) Kutzelnigg, W.; Fleischer, U.; Schindler, M. In *NMR Basic Principles and Progress*; Springer-Verlag: Berlin, 1990; Vol. 23, pp 165−262.
(38) (a) Mann, B. E. In *Transition Metal Nuclear Magnetic Resonance*; Pregosin, P. S., Ed.; Elsevier: Amsterdam, 1991; Vol. 13, pp 177−215. (b) Benn, R.; A., R. *Angew. Chem., Int. Ed. Engl.* **1986**, *25*, 861.
(39) McQuarrie, D. A. *Statistical Thermodynamics*; Harper and Row: New York, 1973.
(40) (a) Bader, R. F. W. *Chem. Rev.* **1991**, *91*, 893−928. (b) Bader, R. F. W. *Atoms In Molecules. A Quantum Theory*; Clarendon Press: Oxford, 1990.
(41) Reed, A. E.; Curtiss, L. A.; Weinhold, F. *Chem. Rev.* **1988**, *88*, 899−926.
(42) Wiberg, K. *Tetrahedron* **1968**, *24*, 1083−1096.
(43) (a) Frisch, M. J.; Trucks, G. W.; Schlegel, H. B.; Scuseria, G. E.; Robb, M. A.; Cheeseman, J. R.; Zakrzewski, V. G.; Montgomery, J. A.; Stratman, R. E.; Burant, J. C.; Dapprich, S.; Millam, J. M.; Daniels, A. D.; Kudin, K. N.; Strain, M. C.; Farkas, O.; Tomasi, J.; Barone, V.; Cossi, M.; Cammi, R.; Mennucci, B.; Pomelli, C.; Adamo, C.; Clifford, S.; Ochterski, J.; Petersson, G. A.; Ayala, P. Y.; Cui, Q.; Morokuma, K.; Malick, D. K.; Rabuck, A. D.; Raghavachari, K.; Foresman, J. B.; Cioslowski, J.; Ortiz, J. V.; Baboul, A. G.; Stefanov, B. B.; Liu, C.; Liashenko, A.; Piskorz, P.; Komaromi, I.; Gomperts, R.; Martin, R. L.; Fox, D. J.; Keith, T.; Al-Laham, M. A.; Peng, C. Y.; Nanayakkara, A.; Gonzalez, C.; Challacombe, M.; Gill, P. M. W.; Johnson, B. G.; Chen, W.; Wong, M. W.; Andres, J. L.; Gonzales, C.; Head-Gordon, M.; Replogle, E. S.; Pople, J. A. *Gaussian 94*,B.2; Gaussian, Inc.: Pittsburgh, PA, 1998. (b) Frisch, M. J.; Trucks, G. W.; Schlegel, H. B.; Gill, P. M. W.; Johnson, B. G.; Robb, M. A.; Cheeseman, J. R.; Keith, T.; Petersson, G. A.; Montgomery, J. A.; Raghavachari, K.; Al-Laham, M. A.; Zakrzewski, V. G.; Ortiz, J. V.; Foresman, J. B.; Cioslowski, J.; Stefanov, B. B.; Nanayakkara, A.; Challacombe, M.; Peng, C. Y.; Ayala, P. Y.; Chen, W.; Wong, M. W.; Andres, J. L.; Replogle, E. S.; Gomperts, R.; Martin, R. L.; Fox, D. J.; Binkley, J. S.; Defrees, D. J.; Baker, J.; Stewart, J. J. P.; Head-Gordon, M.; Gonzales, C.; Pople, J. A. *Gaussian98*; Gaussian, Inc.: Pittsburgh, PA, 1998.

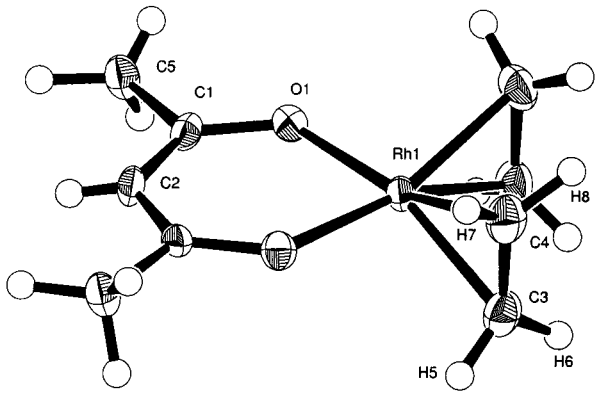

1

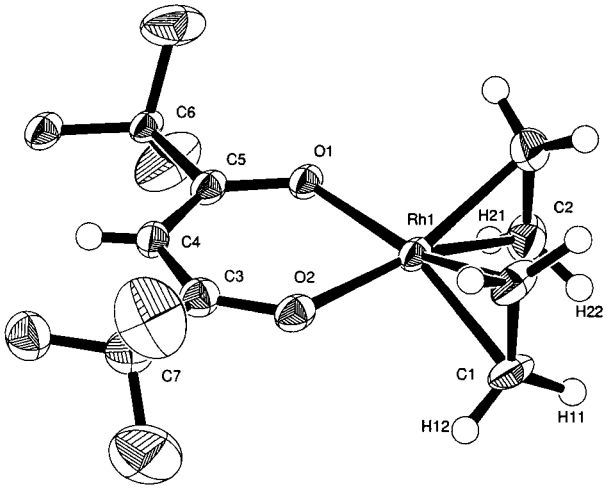

2

Figure 1. Thermal ellipsoid plots of Rh(acac)(ethene)$_2$, **1**, and Rh(hfacac)(ethene)$_2$, **2**. Atoms are drawn at the 50% probability level.

except when fluorine-containing species were involved. For instance, the enthalpy for exchanging both ethenes in **1** with two TFE molecules was computed to be −11.8 and +4.3 kcal/mol at BP86/ECP1 and B3LYP/II, respectively. Since the latter value was obtained with the larger basis set and appeared to be more consistent with experiment (vide supra), only the B3LYP/II data are included in Table 5 and discussed in the following. For the whole series of complexes the calculated ^{103}Rh NMR chemical shifts, Rh−C distances, alkene distortion angle, and elongation af the alkene double bond are given in Table 6.

To investigate the influence of the geometry on the metal shift, the ^{103}Rh NMR chemical shift for Rh(acac)(ethene)$_2$ was computed for several fixed Rh−ethene distances (employing the BP86/ECP1 optimized values for all remaining parameters), and a linear correlation was found. A large Rh−C bond-length shift derivative $\partial[\delta(^{103}\mathrm{Rh})]/\partial[\mathrm{Rh-C}]$ of 10 300 ppm/Å was obtained, quite similar to the corresponding value for the Rh−P bonds in Rh(acac)$(PH_3)_2$.[15] In the same manner, variation of the Rh−acac distance afforded a Rh−O bond-length shift derivative of 4100 ppm/Å.

(44) Popelier, P. L. A. *Comput. Phys. Commun.* **1996**, *93*, 212−240.

Discussion

Geometry of Coordinated Ethenes. The crystal structures of Rh(acac)(ethene)$_2$ and Rh(hfacac)(ethene)$_2$ are very similar, the largest difference between the two structures being the packing and the different symmetries of the molecules. It seems though, that the Rh−O distance is somewhat longer for the hfacac compound **2** than for the acac compound **1**. The Rh−ethene geometries are identical within the experimental error and agree well with those in other complexes containing the Rh(acac)(ethene) unit.[45] An X-ray-derived geometry of Rh(acac)(ethene)$_2$ has been reported before,[5a] but the present structure determination is much more precise since the standard deviations are typically lower by a factor of 4, and all the hydrogen atoms have been located.

When comparing the assembled low-temperature structures of Rh(I)−ethene complexes, as available in the Cambridge Crystallography Database,[46] one finds a weak inverse correlation between the C═C and Rh−C bond lengths (linear correlation coefficient = 0.82, 17 points). However, the relation between longer C═C bonds and decreased *trans*-HCCH dihedral angles, expected from the Dewar−Chatt−Duncanson theory,[6] is absent, probably (but see below) due to the large error in the hydrogen positions so close to the rhodium atom. The reported *trans*-HCCH dihedral angles vary between 150° and 180°.

Upon inspection of the DFT-optimized parameters in Table 6, one notes that the computed C═C bond elongation (for all alkenes, not only ethene) upon complex formation is remarkably constant. Only in the TFE complexes **7** and **9** are shorter RhC bonds paralleled by noticeably increased ΔC═C values. For the whole set of compounds in Table 6, there is also no correlation between Rh−C distances and RCCR′ dihedral angles, even when the chelating diolefins **11**−**13** are excluded. For the "normal" olefin complexes **1**−**5** and **10**, an inverse correlation between these two parameters is obtained, and only for the fluorinated derivatives **6**−**9** is the expected trend apparent.

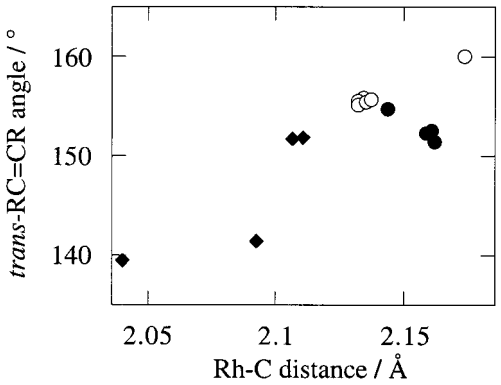

Figure 2. Calculated *trans*-HCCH, -HCCR, or -RCCR dihedral angles plotted against the calculated Rh−C distances for compounds **1** and **3**−**10**: (○) ethenes; (◆) fluoroalkenes; (●) alkylalkenes.

Comparison of X-ray and DFT Structures. In general the agreement is good, angles almost within the

(45) (a) Barlow, J. H.; Curl, M. G.; Russell, D. R.; Clark, G. R. *J. Organomet. Chem* **1982**, *235*, 231. (b) Alcock, N. W.; Brown, J. M.; James, A. P. *Acta Crystallogr., Sect. C* **1989**, *45*, 734.

Table 4. Selected Bond Lengths [Å] and Angles [deg] for the DFT Calculations on 1 and 2 (BP86/ECP1 level) and Mean Values from the Corresponding X-ray Structures (Tables 2 and 3)

	1		2			1		2	
	DFT	exp	DFT	exp		DFT	exp	DFT	exp
Rh−O	2.067	2.051	2.073	2.070	O−Rh−O	91.8	90.9	91.5	90.0
Rh−C	2.132	2.127	2.136	2.124	C−Rh−C same et	38.5	37.6	38.6	37.7
O−C	1.293	1.279	1.282	1.255	C−Rh−C diff et	89.9	89.7	89.7	89.0
C═C	1.407	1.372	1.406	1.392	Rh−C−H outer	106.9	109.3	106.6	107.2
C−CX_3	1.519	1.512	1.543	1.534	Rh−C−H inner	112.7	110.5	112.5	113.6

Table 5. Calculated Energetics (B3LYP/II) for the Exchange of One or Both Ethenes for Another Alkene in Rh(acac)(ethene)$_2$ Compared to Experimental Data[a]

no.	olefin[b]	ΔE [kcal/mol]	ΔH^{298} [kcal/mol]	ΔH_{exp} [kcal/mol]	ΔG^{298} [kcal/mol]	ΔG_{exp}^{298} [kcal/mol]
3	propene	2.3	2.5	1.4 ± 0.9	3.9	1.5 ± 1.1
4	*cis*-butene	4.1	4.0	1.8 ± 0.8	5.6	3.3 ± 1.7
5	*trans*-butene	5.3	5.4	1.9 ± 0.7	6.7	3.7 ± 1.5
6	CH_2CHF	2.6	2.4	−1.6 ± 1.1	3.6	0.6 ± 2.2
7	TFE	−4.9	−5.4		−4.5	−2.7[c]
8	$(CH_2CHF)_2$	5.1	4.8		7.5	
9	$(TFE)_2$	3.0	4.3		6.6	
10	(*cis*-butene)$_2$	8.5	7.8		11.2	
11	COD	0.4	−1.4[d]		−9.7[d]	
12	COT	4.9	2.7[d]		−5.8[d]	
13	NBD	0.1	−2.0[d]		−11.7[d]	

[a] From ref 47. [b] TFE = CF_2CF_2, COD = 1,5-cyclooctadiene, COT = cycloocatetraene, NBD = norbornadiene. [c] Converted from the single measurement of the equilibrium constant K at that temperature. [d] The significant decrease in the ΔG with respect to the ΔH values for the chelating ligands is due to the change of particle numbers in the course of the reaction, reflecting the entropic nature of the chelate effect.

experimental error, although bond lengths tend to be overestimated by around 0.01 Å, as may been expected from gradient-corrected DFT methods. Diffraction methods, on the other hand, tend to underestimate bond lengths because of rocking vibrations.

Some apparent effects in the X-ray structures are not statistically significant. However, the calculations confirm a few details, i.e., there is indeed a small increase in Rh−O bond lengths going from acac to hfacac, the Rh−ethene geometry is identical within 0.004 Å, and the differences in Rh−C−H angles for inner and other ethene hydrogens are indeed real.

Interestingly, while **1** is a true minimum at the BP86/ECP1 level in C_{2v} symmetry, **2** has two very small imaginary frequencies corresponding to rotations of the CF_3 groups. The true minimum on the potential energy surface has C_2 symmetry with the CF_3 groups rotated by ca. 6° relative to their positions in the C_{2v} form. Both C_{2v} and C_2 structures have virtually the same energy, but the former is slightly favored by the zero-point energy (by 0.1 kcal/mol at BP86/ECP1). Obviously, the potential for rotation about the C−C(F_3) bond is very flat, consistent with the observation that the CF_3 groups in hfacac complexes are frequently disordered or show large amplitudes (cf. Figure 1).

We also note that the DFT-derived parameters of Rh(acac)(TFE)(ethene) (Table 6) agree reasonably well with those from X-ray crystallography, Rh−C(TFE) = 2.01 ± 0.03 Å and Rh−C(ethene) = 2.19 ± 0.03 Å,[5a] although the experimental standard deviations in this case are large.

Relative Binding Energies of the Alkenes. In 1967 Cramer measured the stability constants for the exchange of an ethene for another alkene in Rh(acac)(ethene)$_2$.[47] He did this at just two temperatures, 25 and 0 °C, and the so derived enthalpy and entropy values are therefore qualitative only. However, they seem to be the only experimental values available to date. As far as the absolute ΔG and ΔH values are concerned, the accord between computation and experiment is only fair, with deviations up to 4 kcal/mol (Table 5). While errors this large can occur with present-day functionals, one would have hoped for a higher accuracy of the theoretical results due to error cancellation in the isodesmic equations considered. Nevertheless, it is reassuring that the relative sequence for complexes **3**−**6** is the same in both data sets, which gives confidence that the remaining DFT values in Table 5 are at least qualitatively correct.

The remarkable thermodynamic stability of the mono-TFE complex **7** is well reproduced computationally. Substitution of the second ethene by TFE in **7** is calculated highly endothermic, in bearing with the observation that only one ethene in **1** can be replaced by TFE. Kinetic effects, however, may also contribute to the resistance of ethene in **7** against substitution since the replacement of one ethylene for TFE is already much slower than the exchange with other alkenes.[47] Moreover, *cis*-butene readily replaces two ethenes in **1** despite an even larger, computed endothermicity (ca. 11 kcal/mol, entry **10** in Table 5). Even though the latter value is probably overestimated to a large extent, it is clear that the bis(butene) complex is formed against a substantial driving force, which certainly is only possible by removal of ethene from the (rapid) equilibrium during preparation (repeated dissolution of **1** in *cis*-butene and evaporation of volatiles).

^{103}Rh NMR Chemical Shifts and Shifts Correlations. Linear correlations between ^{103}Rh NMR chemical shifts and the overall stability constants were reported for both Rh(I) and Rh(III) complexes in 1994.[16,17] A subsequent review of data in the literature showed similar correlations for other types of rhodium compounds as well as for platinum and cobalt. It was also shown that a linear equation could be derived from the Ramsey equation[48] and crystal field theory, provided that bond enthalpy changes and the $1/\Delta E$ factor were controlling the equilibrium and the chemical shift, respectively.[18] Four Rh(acac)(ethene)(olefin) complexes (**1**, **3**−**5**) appeared to form such a correlation, with the TFE complex **6** lying outside. Correlations between transition-metal chemical shifts and rate constants or catalytic activities have been reproduced and predicted computationally,[10,12,49] and we were interested to explore

(46) Allen, F. H.; Kennard, O. *Chem. Des. Autom. News* **1993**, *8*, 31−37.
(47) Cramer, R. *J. Am. Chem. Soc.* **1967**, *89*, 4621−4626.
(48) (a) Ramsey, N. F. *Phys. Rev.* **1950**, *78*, 699, (b) Mason, J. *Chem. Rev.* **1987**, *87*, 1299−1312.
(49) Bühl, M. *Organometallics* **1999**, *18*, 4894−4896.

Table 6. Experimental and Calculated ^{103}Rh NMR Chemical Shifts and Other Calculated Properties for Rh(acac)(ethene)(alkene), Compounds 3−7, Rh(acac)(alkene)$_2$, 8−10, and Rh(acac)(dialkene), 11−13

		DFT geometries				DFT ^{103}Rh chemical shifts[d] [ppm]				exptl
no.	alkene	Rh−C[a] [Å]	Rh−O[a] [Å]	RCCR′ [deg][a,b]	ΔC=C[c] [Å]	δ_{11}	δ_{22}	δ_{33}	δ_{iso}	δ^{103}Rh [ppm]
1	ethene	2.132	2.067	155.8	0.074	5518	−523	−1775	1074	1170
(**2**[e]	ethene[e]	2.136	2.073	156.4	0.072	5807	−691	−1641	1164	1296)
3	propene	2.141 ± 0.016	2.075 ± 0.003	154.7 ± 4.1	0.073	5546	−391	−1672	1161	1262
		2.130 ± 0.002		155.4 ± 1.0	0.075					
4	*cis*-butene	2.157	2.082 ± 0.004	152.5	0.074	5781	−335	−1614	1277	1353
		2.130		155.1	0.075					
5	*trans*-butene	2.155 ± 0.006	2.079 ± 0.004	152.3 ± 9.9	0.073	5751	−210	−1603	1312	1386
		2.133 ± 0.002		155.4 ± 0.2	0.074					
6	CH_2CHF	2.106 ± 0.013	2.072 ± 0.001	151.7 ± 1.6	0.077	5130	−236	−1746	1049	na
		2.135 ± 0.007		155.7 ± 0.6	0.074					
7	TFE	2.044	2.081 ± 0.013	139.5	0.100	4318	482	−1456	1115	1171
		2.169		160.0	0.066					
8	$(CH_2CHF)_2$	2.110 ± 0.018	2.071	151.8 ± 1.9	0.077	4747	8	−1645	1037	na
9	$(TFE)_2$	2.093	2.090	141.4	0.096	3721	997	−918	1230	na
10	(*cis*-butene)$_2$	2.158	2.091	151.4	0.075	6098	−278	−1341	1493	1509
11	COD	2.129 ± 0.010	2.068	157.9 ± 1.9	0.075	5753	−508	−1350	1298	1306
12	COT	2.130	2.060	157.6	0.068	6675	−372	−958	1780	1760
13	NBD	2.128	2.061	162.1	0.076	6413	−669	−1202	1514	1501[f]

[a] For unsymmetrically substituted complexes, the value for the higher olefin is given first, that for ethene second; when not identical by symmetry, mean values are reported, together with deviations from this average. [b] Dihedral angle of *trans*-substituents at coordinated olefin. [c] C=C bond elongation with respect to free olefin. [d] Tensor components, δ_{ii}, and isotropic shift, δ_{iso}. [e] hfacac ligand. [f] Six, C.; Ph.D. Thesis, University of Jena (Germany), 1997.

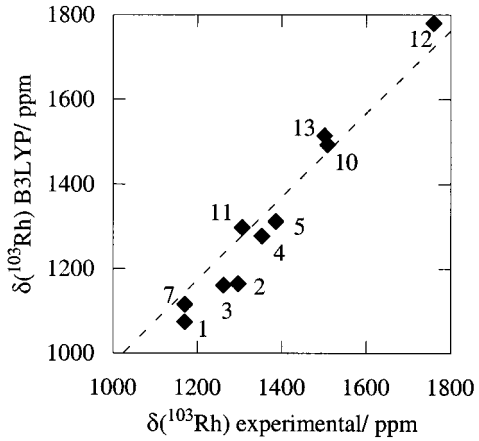

Figure 3. Calculated (GIAO-B3LYP/II) versus experimental ^{103}Rh NMR chemical shifts for (pentanedionato)-rhodium−olefin complexes; dotted line: fit of all Rh compounds computed so far (data from refs 9, 14, and 15; slope 0.98, intercept −3.0).

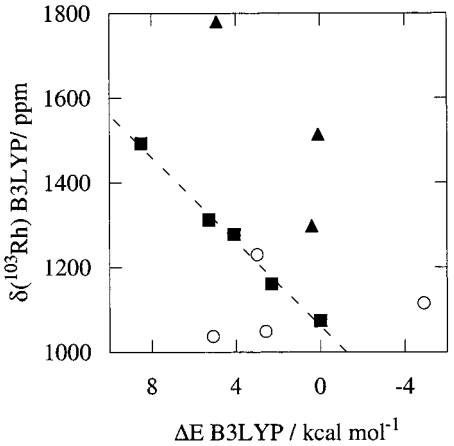

Figure 4. Calculated ^{103}Rh NMR chemical shifts versus calculated alkene binding enthalpy differences: (■) olefins; (▲) diolefins; (○) fluoro-olefins.

if this empirical NMR/stability correlation could be properly described and rationalized theoretically.

For a large variety of Rh compounds, experimental $\delta(^{103}\text{Rh})$ values are very well reproduced at the GIAO-B3LYP/II level, with an accuracy of typically better than 100 ppm (in a range approaching 4000 ppm).[9,14,15] The Rh(acac)(olefin)$_2$ complexes of this study are no exception (Table 6, see Figure 3 for a graphical representation). Thus, predictions should be reliable in cases where a complex or its ^{103}Rh NMR spectrum is not yet known.

In Figure 4 the theoretical (B3LYP) stabilization energies ΔE from Table 5 are plotted against the chemical shifts from Table 6. Clearly, no common correlation is apparent for all species **1** and **3**−**13**. For the subset of nonfluorinated mono-olefins, however, the empirical correlation is nicely recovered and is extended to the bis(*cis*-butene) complex **10**. This correlation can be rationalized in terms of steric effects: Substitution of ethene in **1** with bulkier olefins makes the complexes less stable, as evidenced by increased Rh−olefin distances (Tables 5 and 6). The large sensitivity of $\delta(^{103}\text{Rh})$ toward this parameter is responsible for the concomitant deshielding of the metal. More quantitatively, on going for instance from the bis(ethene) **1** to the bis(*cis*-butene) complex **10**, the Rh−C bond length increases by 0.026 Å (Table 6). Together with the computed Rh−C bond-length shift derivative of **1**, 10300 ppm/Å, an expected deshielding of 281 ppm can be estimated, which amounts to 67% of the actual, computed shift difference between **1** and **10** (Table 6). Similar steric arguments have been put forward to rationalize an empirical NMR/reactivity correlation involving alkyliron compounds.[50] Substitution of ethene in **1** results not only in increased Rh−olefin distances but also in larger Rh−acac separations (Table 6). Due to the sizable Rh−O bond-length shift derivative of 4100 ppm/Å, this Rh−acac elongation can also account for a substantial part of the observed deshielding. On going from **1** to **10**, the 0.024 Å increase

(50) (a) Meier, E. J. M.; Kozminski, W.; Linden, A.; Lustberger, P.; Philipsborn, W. v. *Organometallics* **1996**, *15*, 2469−2477. (b) Bühl, M.; Malkina, O. L.; Malkin, V. G. *Helv. Chim. Acta* **1996**, *79*, 742−754.

in the Rh−O distance corresponds with an estimated deshielding of 98 ppm, or 23% of the actual computed value.

Complexes **6**−**9**, bearing fluorinated olefins, do not fit into the NMR/stability correlation, as has already been observed for the TFE complex **7**. Even though **7** is stabilized appreciably over **1**, both have almost the same ^{103}Rh chemical shift (Table 6). Inspection of the computed individual tensor components, however, reveals larger differences between the two compounds than are apparent from the isotropic values, δ_{iso}. The (δ_{11}, δ_{22}, δ_{33}) values of **1** and **7** are (5518, −523, −1775) and (4318, 482, −1456), respectively. Thus, both span and anisotropy of the shift tensor are considerably reduced upon TFE coordination, but this is not reflected in δ_{iso}. Indeed, compairing all species, three of four fluorinated derivatives have positive, and even large, δ_{22} values, as opposed to the negative values of all other compounds. In addition, the usual relation between bond length and bond strength does not seem to apply to the fluoro-olefin complexes: all have shorter Rh−C distances than the parent **1**, but are, except **7**, computed to be less stable. There are precedents for longer but stronger bonds in the literature.[51]

Similarly, the diolefin complexes **11**−**13** have Rh−C bond distances close to that in **1**, but show larger variations in the stabilization energies. In particular, the ΔE value of the COT complex **12** stands out, +4.9 kcal/mol (Table 5). It appears that strain in the coordinated olefin comes into play: while it costs only 7.5 kcal/mol to distort free ethylene to its geometry in the Rh(acac)complex **1**, 19.4 kcal/mol is released upon relaxing the COT ligand from its structure in **12** (BP86/ECP1 level). It comes therefore as no surprise that the data points for **11**−**13** do not fit into the correlation in Figure 3. Apparently this correlation is only valid for normal, unstrained olefins where steric effects govern both stabilities and ^{103}Rh chemical shifts, and it breaks down when one or the other is dominated by strain or electronic effects.

Electronic Structure of Rh−Olefin Complexes. Which factors determine these electronic effects of fluorinated olefins? The bonding between a transition metal and an olefin is usually interpreted in terms of the Dewar−Chatt−Duncanson (DCD) model,[6] i.e., based on σ-donation from the olefin to the metal and π-back-donation vice versa. The higher stability of the TFE complex **7** with respect to **1** has been rationalized by increased π-back-donation to the more electrophilic fluoro-olefin.[16] In view of the π-complex vs metallacycle dichotomy it was also suggested that "the formulation of Rh−tetrafluoroethylene complexes as metallacyclopropanes would explain some experimental observations".[16]

Topological analysis of the total electron density according to Bader's atoms-in-molecules theory has emerged as a useful probe for the electronic structure of metal−olefin complexes.[52−54] A single bond path from the metal to the midpoint of the olefin is found in case of pure σ-donation; two inwardly curved bond paths from the metal to each of the coordinated olefinic carbon atoms appear as result of significant π-back-donation, and outwardly curved bond paths or similar M−C and C−C bond orders are indicative of a metallacycle. For Ni(COD)$_2$, the DCD model has recently received support from a topological analysis of the experimental electron density using these criteria.[54]

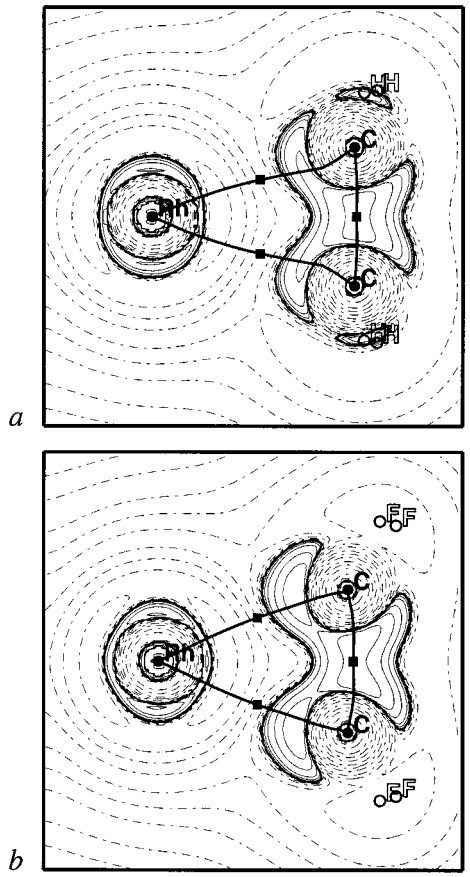

Figure 5. Topological analysis of the B3LYP/II electron density in Rh(acac)(C_2H_4)(TFE): bond paths and Laplacian $-\nabla\rho$ in the Rh−CC(ethene) (top) and Rh−CC(TFE) planes (bottom); contour lines are at $\pm 2^n \times 10^i$ au (n = 1,2,3; i = 2, 1, ..., −3).

The results of the topological analysis of the B3LYP/II density for **7**, which contains both ethene and TFE ligands, are displayed in Figure 5. Clearly, the bonding modes of the two olefins are different. While the Rh−ethene moiety shows the DCD-typical inwardly curved bond paths (Figure 5a), those of the Rh−TFE fragment are curved to the outside (Figure 5b; similar respective pictures are obtained for **1** and **10**). Note also the extrema of the Laplacian ($-\nabla\rho$) between Rh and the carbon atoms in Figure 5b, revealing valence-shell charge concentrations outside the three-membered ring. Together with the very short Rh−C separations and the *trans* FC═CF dihedral angle (139.5°) close to the expected value for a cyclopropane-like structure (140°),[55] these observations support the formulation of the Rh−TFE unit as metallacyclopropane.

(51) For Ti−P bonds, see: Ernst, R. D.; Freeman, J. W.; Stahl, L.; Wilson, D. R.; Arif, A. M.; Nuber, B.; Ziegler, M. L. *J. Am. Chem. Soc.* **1995**, *117*, 5075.

(52) (a) Kulkarni, S. A.; Koga, N. *Theochem-J. Mol. Struct.* **1999**, *462*, 297−310. (b) Böhme, M.; Wagener, T.; Frenking, G. *J. Organomet. Chem.* **1996**, *520*, 31−43.

(53) Frenking, G.; Pidun, U. *J. Chem. Soc., Dalton Trans.* **1997**, 1653.

(54) Macchi, P.; Proserpio, D. M.; Sironi, A. *J. Am. Chem. Soc.* **1998**, *120*, 1447−1455.

(55) A search in the Cambridge Crystallography Database (46) gave values of around 140° for cyclopropane-type structures; see for example entries: ACBCPR, ACCCYP, ACMYCR, ACOHKT, ACXBDO.

However, another way of analyzing the interaction, via Wiberg bond orders,[42] is not as conclusive: at the B3LYP/II level, the Rh−C bond orders in the Rh−ethene and Rh−TFE moieties are 0.4 and 0.6, respectively, and the corresponding CC bond orders are 1.5 and 1.2, respectively.[56] For both ligands, the Rh−C and C−C bond orders are quite different and are not close to unity, as expected for a true metallacycle (as found, for example, in $WCl_4(C_2H_4)$.[53,57] Nevertheless, an enhanced covalent binding of TFE vs ethene is apparent. TFE complexes may thus be considered to be at the borderline between olefin complexes and metallacycles, as the metal−TFE unit is characterized by a more metallacyclopropane-like electron distribution, but not by fully covalent single bonds.[58] This classification is probably not restricted to the systems of this study, but may also be transferable, according to preliminary calculations, to other transition-metal−TFE complexes as well.

This rehybridization is somewhat reminiscent of the increased contribution of the metallacyclopentene structure in the series of Fe, Ru, and Os(1,3-butadiene)$(CO)_3$ complexes, as indicated by the variation of the $^1J_{CH}$ coupling constants.[59] In this context we also note that the $^1J_{CF}$ coupling constant for **7**, 320.4 Hz,[60] is closer to the value obtained for hexafluorocyclopropane, 329.0 Hz, than to that in other fluorinated olefins, e.g., 288.0 Hz for $CF_2{=}CH_2$, although a large variation with substituent can be expected, e.g., $^1J_{CF}$ (CFH_3) = 157.5 Hz and $^1J_{CF}$ (CF_4) = 259.2 Hz.[61] Also olefin rotation has been used as an indication of metallacycles, and this issue has been addressed by Hughes et al.[62]

Conclusion

The DFT calculations describe the Rh−alkene complexes well when compared with the low-temperature X-ray data. Furthermore, when both calculations and experiment are considered together, a more detailed picture of the structures can be obtained, i.e., hydrogen positions have a high experimental uncertainty but are corroborated by theory.

The empirical metal-shift−stability correlation is reproduced by the calculations, but the applicability range of this linear relation is narrowed down somewhat: For normal mono-olefins, the trend toward larger $\delta(^{103}Rh)$ values with lower relative alkene binding energy can be rationalized in terms of steric effects. When strain or electronic effects come to the fore, as in chelating diolefins or in fluoroalkenes, no metal-shift−stability correlation can be expected. The anisotropy of the Rh-chemical shifts are shown to be important in some cases; that is, very close chemical shift values do not necessarily mean electronically very similar rhodium ions.

Topological analysis of the total electron density presents itself as a useful tool to study the electronic structure of transition-metal−olefin complexes. This analysis has revealed qualitatively different binding modes of ethene and tetrafluoroethene to rhodium. Complexes of the latter two can be viewed as being on the borderline between π-complexes in the Dewar−Chatt−Duncanson scheme and true metallacyclopropanes.

Acknowledgment. L.Ö. thanks the Swedish Research Council for Engineering Sciences and Stiftelsen för Strategisk Forskning for financial support. M.B. wishes to thank Prof. Dr. W. Thiel for his continuous support and the Deutsche Forschungsgemeinschaft for a Heisenberg fellowship. M.H. thanks the Swedish Research Council for Natural Sciences. Calculations have been carried out on a Silicon Graphics PowerChallenge (Organisch-chemisches Institut, Universität Zürich) and on Compac XP1000 and ES40 workstations (Max-Planck-Institut Mülheim). We thank W. Leitner for communicating a $\delta(^{103}Rh)$ value.

Supporting Information Available: Listings of crystallographic data. This material is available free of charge via the Internet at http://pubs.acs.org.

OM000419Y

(56) For comparison, the Wiberg bond orders in cyclopropane and hexafluorocyclopropane are 1.0 and 0.9, respectively, at the same level.

(57) For this molecule, Frenking and Pidun report bond orders of 0.9 (W−C) and 1.1 (C−C), obtained with a different theoretical approach. The corresponding Wiberg bond orders at the BP86/ECP1 level are very similar, 0.8 and 1.1, respectively. Thus, the qualitative conclusions drawn here should not depend on the particular quantum-chemical methodology.

(58) (a) Cioslowski, J.; Mixon, S. T. *J. Am. Chem. Soc.* **1991**, *113*, 4142−4145. (b) Bond orders n can also be estimated from the density ρ_{bcp} at the bond critical points according to the equation $n = \exp(A(\rho_{bcp} - B))$, where A and B are fitted to yield $n = 1$ and 2 from the ρ_{bcp} values of ethane and ethene, respectively, cf. ref 40. The C−C bond orders obtained this way for **7** are very similar for both ethene and TFE ligands, around 1.5, and the difference in the corresponding Rh−C bond orders, 0.4 and 0.5, respectively, is less pronounced. As has been pointed out elsewhere,[58a] this approach can be problematic when different types of atomic pairs are involved. In fact, for the aforementioned metallacyclopropane $WCl_4(C_2H_4)$, the same procedure yields W−C and C−C bond orders of 0.4 and 1.3, respectively (BP86/ECP1 level), and appears thus to be less suited to describe covalent bond orders in the systems under scrutiny.

(59) Adams, C. M.; Cerioni, G.; Hafner, A.; Kalchauser, H.; Philipsborn, W. v.; Prewo, R.; Schwenk, A. *Helv. Chem. Acta* **1988**, *71*, 1116, and references therein.

(60) Experimental data as reported in ref 16.

(61) Breitmaier, E. *Carbon-13 NMR spectroscopy: high-resolution methods and applications in organic chemistry and biochemistry*, 3 ed.; VCH: Weinheim, 1987.

(62) (a) Curnow, O. J.; Hughes, R. P.; Rheingold, A. L. *J. Am. Chem. Soc.* **1992**, *114*, 3153−3155. (b) Curnow, O. J.; Hughes, R. P.; Rheingold, A. L. *Organometallics* **1993**, *12*, 3102−3108.